

LASER INTERFEROMETER GRAVITATIONAL
WAVE OBSERVATORY
- LIGO -
CALIFORNIA INSTITUTE OF TECHNOLOGY
MASSACHUSETTS INSTITUTE OF TECHNOLOGY

Document Type LIGO-LIGO-P990001-00-D Jan, 10 1998

**Seismic Noise Filters, Vertical Resonance Frequency
Reduction with Geometric Anti-Springs, a Feasibility Study**

A. Bertolini¹, G. Cella, R. DeSalvo, V. Sannibale
¹*Dept. of Physics, Univ. of Pisa*

Distribution of this draft:
TBD

This is an internal working note
of the LIGO Project.

California Institute of Technology
LIGO Project - MS 18-34
Pasadena, CA 91125
Phone (626) 395-2129
Fax (626) 304-9834
E-mail: info@ligo.caltech.edu

Massachusetts Institute of Technology
LIGO Project - MS 20B-145
Cambridge, MA 01239
Phone (617) 253-4824
Fax (617) 253-7014
E-mail: info@ligo.mit.edu

WWW:<http://www.ligo.caltech.edu/>

Abstract

The achievement of low resonance frequency in vertical action oscillators is the most difficult of the basic ingredients for seismic noise attenuation filters. These oscillations are achieved by means of “anti-springs” systems coupled to more classical suspension springs.

Magnetic anti-springs have been used so far. Geometric anti-springs have been studied and the concept was tested in this work, opening the way to simpler and better performance seismic attenuation filters.

Introduction

Chains of pendula or oscillators of different types are commonly used to depress natural seismic and human generated perturbations on test masses intended to measure gravitational wave signals. Excitations applied to the support of an ideal pendulum are attenuated, limitedly to the pendulum degree of freedom, in a bandpass starting above the pendulum resonance with a well know transfer function $\omega_0^2/(\omega - \omega_0)^2$.

An extended body suspended to a wire is naturally a 5 Degree of Freedom (DoF) oscillator (it can oscillate in the 2 classical pendulum directions, in torque and in the 2 tilt DoF) and therefore attenuates in these five directions. The sixth DoF, i.e. the vertical direction, remains short circuited by the wire rigidity in traction and represent a noise transmission channel to the other DoF. It is then apparent the importance of producing oscillators attenuating simultaneously in all six DoF. This can in principle be obtained by simply suspending an extended body by means of a spring. One may argue that a pendulum suspension wire is itself a spring; the problem is that to hold the weight of the payload it has to be a stiff wire which induces vertical resonances of the order of 100 Hz or higher, too high to be useful in the range of interest of gravitational wave detectors. Soft springs supporting large loads are needed to sufficiently lower the vertical suspension frequency. Moreover, so as not to generate higher order mode up-conversions and internally generated noise larger than what they filter out, springs need to be very clean action and low dissipation ones.

It is useful to mention that in the horizontal direction the resonant frequency is lowered by building longer pendula or inverted pendula[1, 2, 3] or other mechanical techniques of growing complexity[4, 5, 6]. The torsional frequency is naturally low and the two tilt frequencies are easily lowered by hooking a mass close to its center of weight. The Vertical Resonant Frequency (VRF)of suspended bodies has been lowered using folded springs[7], gas springs[8], stiff cantilever springs coupled to Magnetic Anti-Springs (MAS)[9, 10], rubber or composite compression springs[11], magnetic levitation et cetera. All of these techniques have been tested and present major inconveniences or limitations.

Of the best performance systems gas springs are excessively unstable thermally and present nasty stresses and plastic behavior in the bellow welding region. Magnetic anti-springs are very effective but require very complex mechanics. They are quite thermally sensitive and require cumbersome tuning mechanisms and may induce unwanted couplings to external e.m. fields. Some of the above methods have already been abandoned and others may be too if simpler and better performing soft vertical springs can be devised and built.

Magnetic levitation is very promising, but is still being developed.

In this development we tried to improve the weak points of the existing techniques while keeping their strong points. The strong point of the Virgo vertical springs concept is to use strong triangular cantilever springs, optimized to suspend high loads and couple them to an anti-spring system which is designed to locally soften the spring constant, thus reducing the VRF at the working point. The main drawback of this design is that it makes use of a magnetic anti-spring system made with components with different thermal behaviors that generate working point stability problems difficult to control. Also the magnetic anti-springs are intrinsically transversally unstable and must be stabilized with stiff centering wire mechanisms.

Recently the use of torsion bars coupled to rigid levers and flexible links in a Geometric Anti-Spring (GAS) configuration has been suggested[12]. The advantage of an all mechanical system is that it is simpler and much more thermally stable. This approach has a technical problem stemming from the forbidding geometrical requirements of the torsional bars when requiring them to sustain large loads. To satisfy these requirements, the authors have proposed to use composite torsional bars that introduce a lot of complexity to the system and may end up introducing a lot of excess noise.

In this paper we propose the use of triangular cantilever blades, as does VIRGO, coupled to inclined links, as in the Australian proposed torsion bar system, generating the desired geometrical anti-spring effect.

The VIRGO Super-Attenuators filters (SA) are currently made by a crown of converging pre-bent blades which are re-straightened by the load and work purely in the vertical direction. The blades of the present design are flat when unloaded and bent by the load. The blade's base is oriented so that the blade's tip describes an inclined curved trajectory when oscillating around the working point. Counter-inclined wires link each blade's tip to a suspended disk to which the load is attached.

The vertical movement of the disk induces a change of the wire inclination which, in its turn, modulates the projections of the forces acting on and from the wire. It is the interplay of these force projections that generate the desired vertical anti-spring effect. The anti-spring strength can be tuned to match the spring strength by simply changing the disk diameter. The filter kinematics have been extensively studied and optimized in computer simulations and tested in a pre-prototype.

The next four chapters describe the simulation and optimization process, then the prototype tests are discussed along with the requirements for a more meaningful prototype of an effective seismic attenuation filter.

Static Model of a Thin Blade

For the theoretical description of the thin blade, we have adopted the unidimensional model which is adequate to study blades symmetric along one axis (longitudinal axis).

Considering a curvilinear coordinate l along the blade axis of symmetry, and a pre-stressed angular profile $\Omega(l)$, the potential energy of the blade is

$$U(L) = \frac{1}{2} \int_0^L \gamma(l) \left(\frac{d\theta}{dl} - \Omega(l) \right)^2 dl, \quad (1)$$

where L is the blade length, $\gamma(l) = EI(l)/(1 - \sigma^2)$, with E and σ the Young modulus and the Poisson ration of the material and $I(l)$ the local moment of inertia of the blade cross section in l . Ω is the inverse of the radius of curvature of the blade.

With one blade end constrained, the work done by the external force $\vec{F} = (F_x, F_y)$ applied to the other extremity is

$$U_{ext.} = \int_0^L [F_x \cos \theta(l) + F_y \sin \theta(l)] dl. \quad (2)$$

Imposing the equilibrium condition between U and $U_{ext.}$, we obtain the fundamental equation

$$\frac{d}{dl} \left[\gamma(l) \left(\frac{d\theta}{dl} - \Omega(l) \right) \right] = F_x \sin \theta(l) - F_y \cos \theta(l), \quad (3)$$

which gives the static profile of the pre-stressed blade subject to an external force applied to one extremity.

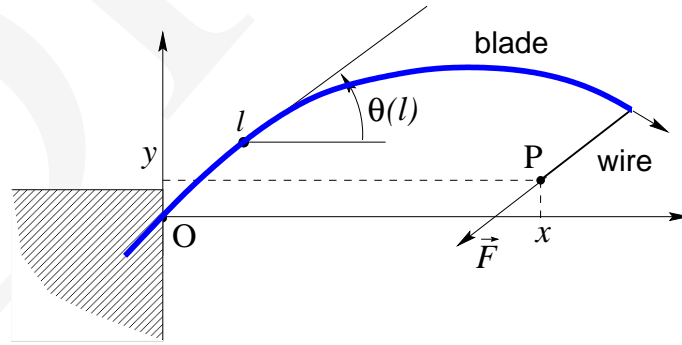


Figure 1: blade reference frame.

We consider a trapezoid blade configuration, with the base rigidly fixed at the origin at a given angle θ_0 , measured from the horizontal axis (see fig.1). The other extremity is subject to an external force \vec{F} transmitted by a wire of length l_w . The coordinates of the other wire extremity P are (x, y) .

For this particular configuration, the boundary conditions are

$$\theta(l = 0) = \theta_0, \quad \left. \frac{d\theta}{dl} \right|_{l=L} = \Omega(L). \quad (4)$$

The initial blade geometry (at $\vec{F} = 0$), the final wire length and its lower extremity coordinates P , that have to be reached at the equilibrium, are imposed. \vec{F} is free to change its magnitude and direction dragging the wire direction towards P and achieve the equilibrium condition. (This algorithm is equivalent to pulling the wire through the point P until it reaches the length l_w .) The equation (3), for a given value of \vec{F} , is a nonlinear boundary value problem, which can be solved numerically using standard integration algorithms.

Computing different geometries, we can find useful working points and optimize the load and the stress of the blade.

The next step is to determine the parameters of the blade for the dynamical description around the equilibrium and in the linear regime.

Quasi-static Model of the Blade

The most general relation to describe the dynamical behavior of the blade extremity in the linear regime is

$$\begin{pmatrix} \delta x(L) \\ \delta y(L) \end{pmatrix} = \begin{pmatrix} m_{xx} & m_{xy} \\ m_{xy} & m_{yy} \end{pmatrix} \begin{pmatrix} \delta F_x \\ \delta F_y \end{pmatrix}, \quad (5)$$

where $\delta F_x, \delta F_y$ are the force components at the extremity and $\delta x(L), \delta y(L)$ the produced displacements.

The matrix coefficients, which depend on the blade geometry at the equilibrium, can be obtained starting from the linearized expression of the (3), by applying a perturbation to the forces and to the blade profile. Labeling all the observables at the equilibrium with the * index and applying to the eq.(3) the following substitutions:

$$\begin{cases} \theta(l) &= \theta^*(l) + \delta\theta(l) \\ F_x &= F_x^* + \delta F_x \\ F_y &= F_y^* + \delta F_y \end{cases}, \quad (6)$$

we obtain the linearized equation of the thin blade around the equilibrium

$$\begin{cases} \frac{d}{dl} \left[\gamma(l) \frac{d\theta}{dl} \right] = \delta F_x \sin \theta^*(l) - \delta F_y \cos \theta^*(l) + F_x^* \delta\theta(l) \cos \theta^*(l) - F_y^* \cos \theta^*(l), \\ \delta\theta(l=0) = \theta_0, \quad \frac{d\delta\theta}{dl} \Big|_{l=L} = 0. \end{cases} \quad (7)$$

With $q_x(l) = \delta\theta(l)/\delta F_x$ and for $\delta F_x \neq 0$ and $\delta F_y = 0$, the previous expression becomes

$$\frac{d}{dl} \left[\gamma(l) \frac{dq_x}{dl} \right] = \sin \theta^* + (F_x^* \cos \theta^* + F_y^* \cos \theta^*) q_x. \quad (8)$$

In the same way, with $q_x(l) = \delta\theta(l)/\delta F_x$ and for $\delta F_x \neq 0$ and $\delta F_y = 0$, we have

$$\frac{d}{dl} \left[\gamma(l) \frac{dq_y}{dl} \right] = -\cos \theta^* + (F_x^* \cos \theta^* + F_y^* \sin \theta^*) q_y. \quad (9)$$

Resolving numerically the eq.s (8) and (9), we can compute the coefficients m_{xx}, m_{yy}, m_{xy} using the following relations obtained from the (5)

$$m_{xx} = - \int_0^L q_x(l) \sin \theta^*(l) dl, \quad (10)$$

$$m_{xy} = \int_0^L q_x(l) \cos \theta^*(l) dl = - \int_0^L q_y(l) \sin \theta^*(l) dl, \quad (11)$$

$$m_{yy} = \int_0^L q_y(l) \cos \theta^*(l) dl. \quad (12)$$

Given that, for the usual description of the dynamical behavior, we are interested in the following expression:

$$\begin{pmatrix} \delta F_x \\ \delta F_y \end{pmatrix} = \begin{pmatrix} k_{xx} & k_{xy} \\ k_{xy} & k_{yy} \end{pmatrix} \begin{pmatrix} \delta x(L) \\ \delta y(L) \end{pmatrix}, \quad (13)$$

the matrix of the eq.(5) has to be inverted.

To complete the dynamical description of the system, we need the relations between the coordinates variations $(\delta x(L), \delta y(L))$ and those $(\delta X, \delta Y)$ of the wire extremity P . At the first order this relations can be obtained considering that the wire length l does not change ($\delta l = 0$) and the the force \vec{F} is always directed along the wire. From these relations, a new matrix of k coefficients that links the force components to the variations $(\delta X, \delta Y)$ can be finally computed.

Results of the One Dimensional Model

In a concentric blade configuration with angularly and equally spaced blades, the linking wires connected to a single central disk, all transversal forces null up. Taking advantage of this fact, in a first round of analysis it was found convenient to consider just the one dimensional case of the vertical motion, treating the transversal stability problem separately. This approximation already cleared up a lot of facts important for the construction of an actual system:

- Given a VRF specification, it is possible to find a solution either near a mechanical bi-stability or at a suitable frequency minimum (see figure 2).

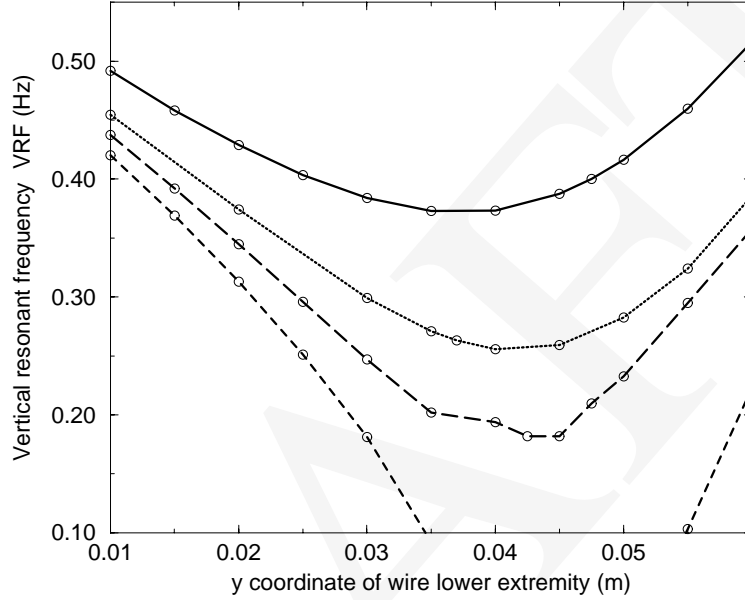


Figure 2: Vertical resonant frequency versus payload vertical position (y in fig.1). Each curve corresponds to a different x coordinate as defined fig.1. The scatter of some points is due to numerical precision errors. The effect of these errors is more visible at low frequencies, where spring and anti-spring add up to a smaller number.

- It is obviously desirable to operate the filter at a frequency minimum because the VRF near a bi-stability varies rapidly; this would result in very limited filter working point dynamic ranges and in very difficult tunability.
- It is easy to generate a filter VRF minimum at the desired frequency by simply changing the relative radial distance between the blade base and the wire hooking point on the suspension disk. As illustrated in figure 2, it is increasingly difficult to achieve the radial positioning precision necessary for the lowest frequency requirements. A 1 mm blade dimensional tolerance allows a factory VRF pre-setting no lower than 200 mHz ($\pm 1 \text{ mm} \rightarrow 200_{-20}^{+50} \text{ mHz}$). It is then unwise to aim for lower VRF GAS filters without a suitable fine tuning mechanism.
- The position of the VRF minimum changes very slowly as a function of its specified value (figure 2).
- The calculated thermal sensitivity of a GAS filter, taking into account the thermal Young's modulus variation and the differential thermal expansion coefficients, is of $-38 \mu\text{m}/^\circ\text{K}$ for the payload height and $0.44 \text{ mHz}/^\circ\text{K}$ for a vertical resonance frequency of 280 mHz.
- The stress distribution along the blade is fairly uniform (figure 3), varying by less than a factor of 2 over most of the blade length. In other terms, the simple triangular

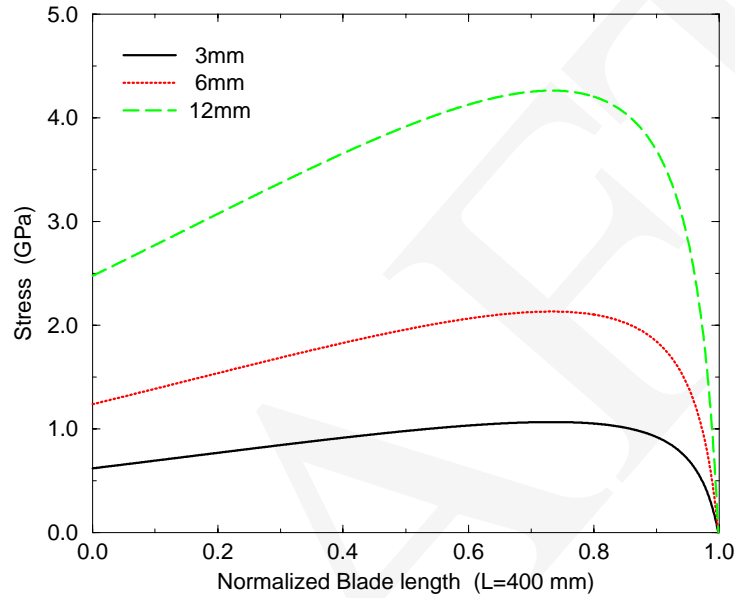


Figure 3: Blade stress along the curvilinear coordinate l normalized to the blade length of 400 mm. The 3 curves correspond to 3 mm (continuous line), 6 mm (dotted line), 12 mm (dashed line) of blade thickness.

geometry is making a rather efficient use of the material strength.

- The stress distribution along the blade length could be further optimized by modifying the triangular blade geometry, making the blade narrower and more loaded at its base. This operation will tend to bring the curvature of the blade under stress closer to a circle. Improving the blade stress profile at its tip has little practical interest due to the small lever arm left.
- Changing the blade thickness neither changes the filter VRF minimum value, nor its vertical positioning, it only changes the filter load capabilities, (which grows as the third power of the thickness) and the amount (but not the distribution) of the stress in the blade, which grows linearly with the thickness. These last two points allow an easy optimization of the material thickness and load factor for a minimization of blade weight and momentum of inertia. Using the thickest possible blade allowed by the stress limitation of the material and by the geometry, it is also important to maximize the blade beam resonant frequencies.
- Blade base inclination and blade pre-stress (its curvature at rest) are largely exchangeable and can be traded to optimize price and geometry. The choice of 45° blade inclination allows the direct use of unstressed (flat) blades while achieving good filter performances.
- It is easy to achieve the necessary anti spring strength without requiring shallow link

wire angles. In most parameter choices the link wire results in being close to perpendicular to the blade tip and more than 30° from the horizontal disk plane. Consequently the amount of force to be transmitted by the wire link is always less than the double of the applied load.

- The angles of the link wire change slowly around the VRF minima thus allowing the use of low dissipation, low excess noise, flex joints.

The scatter of data at very low VRF in figure 2 is due to numerical errors in the cancellation between spring and anti spring forces. It can be eliminated by using finer calculation meshes, but it is indicative of the progressive criticality of lower frequency tuning.

Tri-dimensional Model

In order to understand the transversal stability problem a model connecting a number n ($n > 3$) of equally spaced concentric blades to a central disk, and allowing its six DoF movements was made.

This model allowed us to calculate that:

- The horizontal translation and tilt modes mix substantially.
- The disk has rigid torsion and horizontal quasi-translational modes but very soft quasi-tilt modes.

Although one would be tempted to try to use the horizontal component of the soft quasi-tilt mode for additional horizontal attenuation, it is advisable to impede this mode, for example by means of a set of centering wires.

Prototype Tests

Guided by the simulation, a four blade prototype was designed and built on a modular steel frame; the blade clamps were mounted on rotating and sliding supports to scan both the blades' base inclination with respect to the horizontal plane and their radial distance from the hooking point on the central disk.

In the set-up, the load could be attached to the center of the disk either by means of a rigid rod, impeding all tilting movements of the disk, or by means of a 1.5 mm diameter music wire. The tilting DoF of the suspension disk could be frozen by a tower structure extending 200 mm down from the disk. The bottom of this tower was constrained to the center of the frame by four radial centering wires. A cut view of the prototype is shown in figure 4.

The blade geometry, chosen by the simulation, was a simple isosceles triangle 400 mm high, 104 mm large at the base, 3 mm thick. The blades were not pre-stressed, i.e. they were flat at rest.

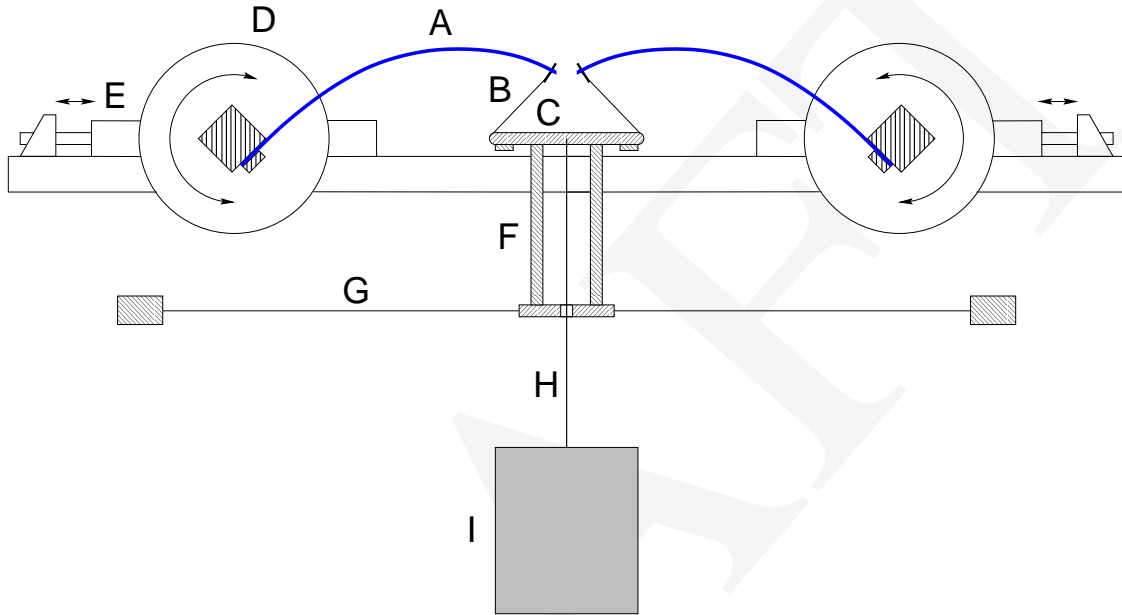


Figure 4: Cut view of the setup for the experimental tests. A: stressed blade, B: link wire, C: load disk, D: angular movement of the blade base, E: radial movement of the blade base, F: anti-tilt tower, G: anti-tilt centering wires, H: suspension wire (or rod), I: load.

No effort was made to make low friction links. To hook the wire to the blade tip a 2 mm diameter hole was drilled where the blade is 4 mm wide and the wire was simply looped 180° around a nail, sticking from the hole and the blade tip itself. The two wire ends were cut at a length of about 100 mm; 80 mm were left between the blade tip and the contact point on the disk, the rest of the wire ends bent around the 5 mm radius edge of the disk and clamped down on it. The resulting links were quite dissipative due to the friction and presented a large amount of hysteresis, but proved good enough to test the kinematics of the system.

The blades were mounted in one of the calculated configurations, i.e. with bases inclined at 45° and a 295 mm horizontal separation between the blade base and the edge of the disk; the filter was loaded with lead bricks.

The load was initially supported by the rigid rod (500 mm long). At about the nominal load of 155 kg the filter showed a bi-stable behavior due to the anti spring overwhelming the spring strength. A stable working point was found by backing off the blade bases by 4 mm in agreement with the prediction of figure 2.

Several curves of frequency vs. vertical disk position were measured for different blades translations (see figure 4) and their behavior, as shown in figure 5, agreed very well with the simulations of figure 2. The experimental points have been obtained by adding small weights (several tens to few hundred grams per step) to a basic payload of 150 kg. The frequency minima positions showed a weak dependence on the blade positioning while the values of the VRF minima showed a rapid decrease (figure 5), also in agreement with simulation

data. As the frequency minimum rapidly decreases if the distance between the blades is reduced, it becomes extremely sensitive to their positioning. Despite the fact that arbitrary low frequencies are theoretically possible, we could not go below minimal frequencies of 200 mHz due to the roughness of the prototype. Below 200 mHz, further blade forward movements resulted in effective spring constants so small that they were overwhelmed by the wire static friction, thus producing indifferent equilibrium points. Eventually excessive forward positioning of the blades induced a bi-stable configuration. After taking into account the hysteresis problem, the agreement between measured and simulated data completely validated the simulation procedure.

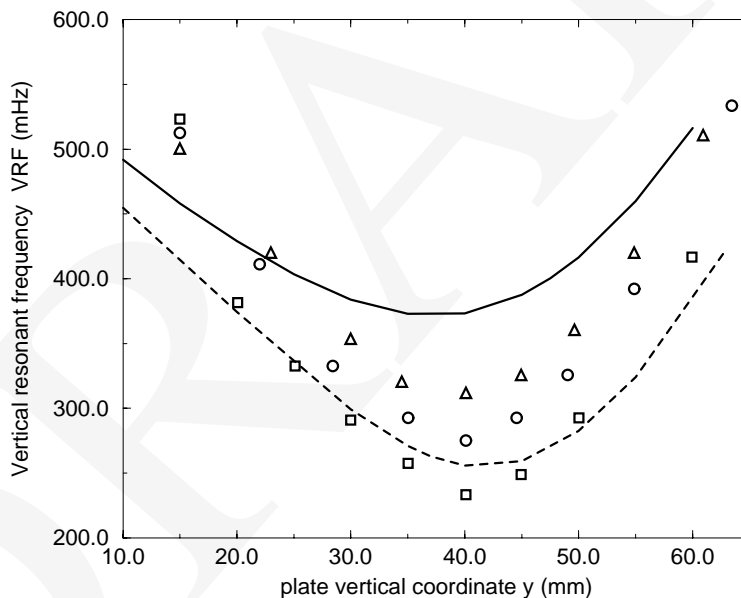


Figure 5: Experimental points obtained measuring the VRF of the 4 blades system changing the vertical coordinate of the plate (the y coordinate of the wire). The different curves correspond to different distances between the plate extremity to the clamped blade extremity (the x coordinate of the wire). Squares $x = (295 \pm 4)$ mm, circles $x = (296 \pm 4)$ mm, triangles $x = (297 \pm 4)$ mm. The dashed and the solid curves correspond to the simulation with $x = 300$ mm and $x = 302$ mm respectively

Tests were then made by replacing the load rod with the flexible wire. The wire attachment point was just below the disk surface. The small differences between the blades immediately introduced a disk tilt which increased when lower oscillation frequencies were tuned but very small forces on the disk were necessary to keep it level. The tilt could also be eliminated by micro-metrically adjusting the blades' bases' angles. This cumbersome and delicate operation is certainly unacceptable in a real life filter working under vacuum, which must be sturdy and reliable. Tests in this configuration were cut short and centering wires were connected to the disk tower to impede its tilting DoF. The centering wires hooking points on the external structure were adjusted so that the four wires laid on a plane at

the vertical position corresponded to minimum vertical frequency. The amount of required AS strength (connected to the blades base movement) was obviously dependent on the wires tensioning (horizontal centering wires in first approximation contribute a vertical spring constant proportional to the tensioning and are inversely proportional to their length) but very little tensioning was necessary to provide stability and little perturbation on the minima and their width was observed¹.

A few other measurements were attempted. The resonant frequency of the torsion mode of the disk was measured by placing a small accelerometer (Kistler 8630C5) on it and observing its spectral response with a FFT spectrum analyzer (Stanford Research SR 780); the resonance was found to be 36 Hz, normally a dangerous frequency due to its location just in the gravitational wave range of interest. It was however found that even extreme excitations of this mode (millimetric oscillations at the periphery of the disk) were not detectable on the payload after the 500 mm long 1.5 mm diameter suspension wire.

The main beam resonances of the blades were excited by means of a home made electromagnetic non-contacting exciter and measured to be at 56 Hz. This vibration was readily transmitted to the disk, with just 20 – 25 dB attenuation measured between two accelerometers placed at the center of the blade and the point of the disk just below the link. This resonance could be simply damped, as in the VIRGO filters; we attempted instead to first null the energy transmission effects of this resonance by adding a small counterweight to the blades' tips. These weights are intended to bring the blade oscillation node to coincide with the wire attachment point. The transfer function was improved by the counterweight by about 10 dB at resonance; fine mass tuning of the counterweight for better reduction was impeded by the many resonances of the support structure, of the disk and of the payload. This improvement has still to be perfected in a more rigid filter structure. After nulling its effects, the blade resonance would be also damped for added performance.

Comments and Conclusions

The Geometric Anti-Springs appear to be a much simpler and better performing device than the magnetic anti-springs; they will have several, some as yet uncharted, repercussions on the filter dynamics.

The weight of the magnet matrices and of their tuning mechanism can be completely spared yielding higher spurious resonances.

Additionally the dynamic range of GAS for a given vertical resonance acceptance is much larger than in MAS, therefore no remote working point sensing and tuning mechanism is required. This simplification is possible also by the fact that the magnets were by far the most thermally sensitive element in the MAS filters and the GAS filters are calculated to be more thermally stable.

¹We estimated the centering wire tension by measuring the frequency of their violin mode by means of a commercial electric guitar pickup and tuner; we adjusted frequencies between 50 and 70 Hz, corresponding to tensioning between 20 and 50 N.

Eliminating the mass of the magnetic anti springs from the moving “equipment” of the filter greatly increase the recoil frequency of the central disk with respect to the underlying filter body caused by the recalling force of the suspension wire. Pushing this resonance at higher frequency will make it less deleterious for the detection bandpass and easier to damp; the smaller recoil mass will store less energy and would require a smaller damper mass with further reduction of weight.

The VRF of the MAS filters can be easily tuned by micro-metrically changing the gap between the magnets. Tuning the GAS is much more difficult because it would require a change in geometry, for example the change of the central disk diameter. The GAS strength will then come factory pre-set and no infield tuning of its strength will be possible. Fine tuning the VRF can still be achieved in GAS filters by pre-setting the GAS to a slightly lower VRF and then tuning it up by increasing the centering wire tensioning. The reduction of VRF dynamic range induced by the higher order components of the centering wires spring constant is small. In all cases GAS filters still present much better dynamic range characteristics than their MAS brothers of similar size.

With the results of these simulations and test we are confident enough to begin the design of a new generation of seismic isolation filters for LIGO, inspired by the VIRGO ones but much simpler and better performing. Several other simplifications and improvements are envisaged.

Instead of tuning the filter’s loading capabilities to the suspended load, the filters would be manufactured for a slight excess of load capability and the load would be matched to it by simply adding some ballast on the following filter body. This simple method will eliminate all the cumbersome load tuning devices on the filter and the unwanted resonances that they would entail.

The blades would not be clamped to the filter body by means of bolts and nuts but rather wedged in suitable slots in the filter outer rim.

The links between the blades and the central disk would not be made by clamped wires. Instead seated hooks ending with flex joints continuing directly into a rectangular section link wire would be used. This solution not only will eliminate all screws on the blades and on the disk, but it is particularly well suited for low dissipation and minimum excess noise.

To further reduce the number of potential excess noise sources in the seismic attenuation chain all electrical wiring should be eliminated.

References

- [1] M. Pinoli, D. G. Blair, L. Ju, *Meas. Sci. Tech.* 4, 995 (1993)
- [2] G. Losurdo et al., **An inverted pendulum pre-isolator stage for VIRGO suspension system**, to be submitted to *Rev. Sci. Instr.*
- [3] P. Saulson, RT Stebbins, FD.Dumont, SE Mock, *Rev. Sci. Instrum.* 65 (1994) 182-191

- [4] M. A. Barton, N. Kanda and K. Kuroda, **A low-frequency vibration isolation table using multiple crossed-wire suspensions**, *Rev. Sci. Instrum.* 67(11) 3994 (1996).
- [5] D. G. Blair, J. Liu, E.F. Moghaddam, L. Ju, **Performance of an ultra low-frequency folded pendulum**, *Phys Lett. A* 193 223 (1964).
- [6] J. Winterflood and D. G. Blair, **A long-period conical pendulum for vibration isolation**, *Phys Lett. A* 222 141 (1996).
- [7] D. G. Blair, L. Ju and M. Notcutt, **Ultra high Q pendulum suspensions for gravitational wave detectors**, *Rev. Sci. Instrum.* 64(7) 1899 (1993).
- [8] R. del Fabbro, A. Di Virgilio, A. Giazotto, H. Kautzky, V. Montelacini and D. Passuello, **Performance of a gas springs harmonic oscillator**, *Rev. Sci. Instrum* 59 293 (1988).
- [9] Beccaria M. et al., **Extending the VIRGO gravitational wave band down to a few Hz: metal blade springs and magnetic anti-springs**, *Nucl. Instr A* 394(3) 397 (1997).
- [10] R. De Salvo et al., **Performances of an Ultra Low Frequency Vertical Pre-Isolator for the VIRGO Seismic Attenuation Chains**, submitted to *Nucl. Review* (1998).
- [11] T. Thompson, W. Miller and E. Ponslet, **PDR/CDR Design Review Document**, *LIGO internal document* LIGO-C970 257-00-D (1997).
- [12] Winterflood and D. G. Blair, **A long-period vertical vibration isolator for gravitational wave detection**, *Phys. Lett. A* 243 1 (1998).